

Simulation of a Calcium Looping CO₂ Capture Process for Pressurized Fluidized Bed Combustion

Benoit Duhoux[†], Robert T. Symonds^{‡,}, Robin Hughes[‡], Poupak Mehrani[†], Edward J. Anthony[§], Arturo Macchi[†]*

[†] Department of Chemical and Biological Engineering, Centre for Catalysis Research and Innovation, University of Ottawa, 161 Louis Pasteur Street, Ottawa, Ontario K1N 6N5 Canada

[‡] Natural Resources Canada, CanmetENERGY, 1 Haanel Drive, Ottawa, Ontario K1A 1M1 Canada

[§] School of Applied Science, Cranfield University, Cranfield, Bedfordshire MK43 0AL, United Kingdom

ABSTRACT

The Canadian regulations on carbon dioxide emissions from power plants aim to lower the emissions from coal-fired units down to those of natural gas combined cycle (NGCC) units. Since coal is significantly more carbon intensive than natural gas, coal-fired plants must operate at higher net efficiencies and implement carbon capture to meet the new regulations. Calcium looping (CaL) is a promising post-combustion carbon capture (PCC) technology that, unlike other capture processes, generates additional power. By capturing carbon dioxide at elevated temperatures, the energy penalty that carbon capture technologies inherently impose on power plant efficiencies is significantly reduced. In this work, the CO₂ capture performance of a calcium-based sorbent is determined *via* thermogravimetric analysis under relatively high carbonation and low calcination temperatures. The results are used in an aspenONE™ simulation of a CaL process applied to a pressurized fluidized bed combustion (PFBC) system at thermodynamic equilibrium. Combustion of both natural gas and coal are considered for sorbent calcination in the CaL process. A sensitivity analysis on several process parameters, including sorbent feed rate and carbonator operating pressure, is explored. The energy penalty associated with the capture process ranges from 6.8 to 11.8 percentage points depending on fuel selection and operating conditions. The use of natural gas results in lower energy penalties and solids circulation rates, while operating the carbonator at 202 kPa(a) results in the lowest penalties and drops the solids circulations rates to below 1000 kg/s.

KEYWORDS: Carbon capture, calcium looping, pressurized FBC, process simulation

* Corresponding author: Robert Symonds, Tel: +1 613 996-5153, Fax: +1 613 992-9335
E-mail address: Robert.Symonds@canada.ca

INTRODUCTION

Fossil fuels represent the major energy source for electricity production in the world. In 2015, approximately 66% of the world production relied on fossil fuel, with coal alone accounting for up to 39% of the global power output.^[1] Whilst energy production predictions foresee a shift towards renewable sources of energy (*e.g.*, solar, hydro, wind, *etc.*), fossil fuels, and coal in particular, will still constitute an important source of energy.^[1] Natural gas represents a cleaner source of energy as it is less carbon intensive,^[2] whereas coal contains more sulphur and generates ash, along with a wide range of micro-pollutants (*e.g.*, halides, mercury). The CO₂ intensity of a process, defined as the amount of CO₂ emitted per unit of net power produced, depends mainly on the fossil fuel burned in the power plant. Average values range from about 400 kg/MW_{eh} for natural gas units to 900 kg/MW_{eh} for coal cases.^[2] Present regulations in Canada require that carbon emissions from existing coal power plants reach natural gas-fired levels by 2030 or the end of their useful life (defined as between 45 and 50 years after commissioning date), whichever comes first. New coal-fired power plants must comply upon start-up.^[3,4] The important difference in current carbon emissions from these two types of power plants will force the implementation of carbon capture and storage (CCS) in coal-fired power plants, in addition to efficiency improvements.

Pressurized fluidized bed combustion (PFBC) is a particular implementation of fluidized bed combustion where the boiler is usually operated between 1 and 1.5 MPa.^[5] By operating at elevated pressures, additional energy recovery *via* latent heat and hot flue gas expansion can be realized, in addition to the steam cycle used in all power plants. This combined cycle results in efficiencies above 40% on a higher heating value (HHV) basis, reducing the carbon intensity of the process.^[5,6] Calcium looping (CaL) is a post-combustion carbon capture technology that uses the reversible carbonation reaction to capture CO₂. The process circulates calcium-based sorbents between two reactors: the carbonator where CO₂ reacts with calcium oxide (Equation (1)); and the calciner where the combustion of a fuel generates the heat necessary to calcine calcium carbonate (Equation (2)). The process is illustrated in Figure 1. Due to sorbent sintering and/or reaction with other species (*e.g.*, SO₂), the conversion of calcium oxide in the carbonator decreases as the sorbent is cycled in the process.^[7,8] To maintain the conversion at a desired level, a make-up of fresh limestone and a purge to remove spent sorbent are implemented. The calciner operates in oxy-combustion mode to avoid the dilution of CO₂ with nitrogen from air and to reduce the energy required for the compression of the calciner outlet gas.

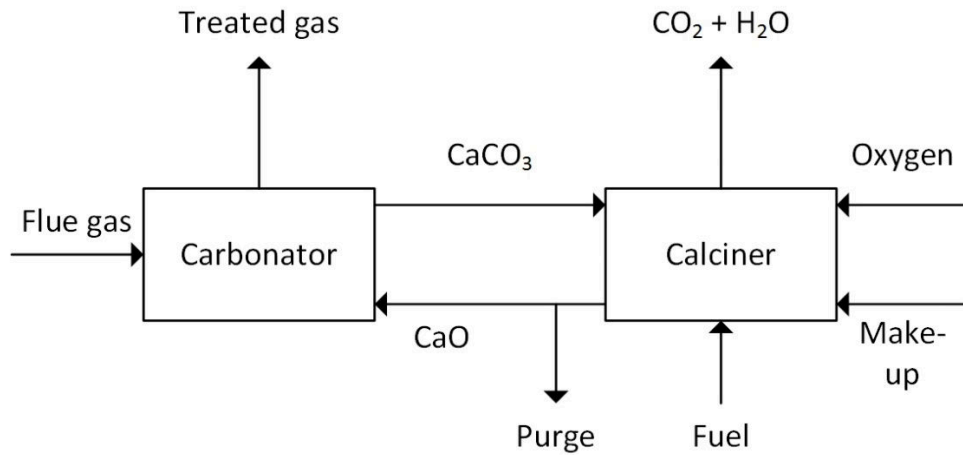
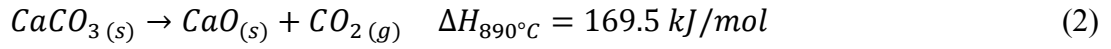
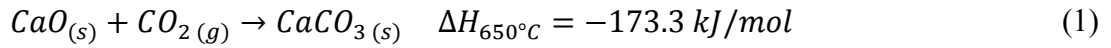


Figure 1: Calcium looping (CaL) block flow diagram.

This work considers the simulation of a CaL process for post-combustion CO₂ capture from a PFBC power plant. Mass and energy balances are performed to investigate the effect of operating parameters on stream characteristics *via* a series of sensitivity analyses. Estimations for the energy penalty of CaL on the base power plant are also provided as an additional comparison criterion. In this investigation, the gross efficiency associated with power production from the carbon capture process is based on previous work on a similar system.^[9] The capture process simulations are based on the cyclic CO₂ sorption of a limestone that was investigated in a series of thermogravimetric analyzer (TGA) experiments. The limestone was subjected to multiple cycles of relatively high-temperature carbonation and low-temperature calcination. These particular conditions were selected in order to minimize the temperature difference between the two reactors in the CaL process and reduce the fuel consumption in the calciner. The use of both natural gas and coal in the calciner was compared by using different gas atmospheres during the calcination step.

MATERIAL AND METHODS

Experimental Methods

The tests were conducted using a naturally occurring Canadian limestone (Cadomin), sieved to a diameter range of between 300 and 425 μm , which is an appropriate size range for circulating fluidized bed operation. The composition of the sorbent, obtained from X-ray fluorescence (XRF), is provided in Table 1.

Table 1: Composition of Cadomin limestone as determined *via* XRF (300 – 425 μm in diameter)

Component	Mass fraction (wt%)
SiO₂	1.44
Al₂O₃	0.3
Fe₂O₃	0.35
TiO₂	<0.03
P₂O₅	<0.03
CaO	52.27
MgO	1.54
SO₃	<0.10
Na₂O	<0.20
K₂O	0.09
Ba	<250 ppm
Sr	258 ppm
V	<50 ppm
Ni	<50 ppm
Mn	80 ppm
Cr	< 50 ppm

Cu	<30 ppm
Zn	<30 ppm
LOF*	43.96

*Loss on fusion

The sorbent was tested using a Cahn 1000 Electrobalance thermogravimetric analyzer, using sample sizes of approximately 20 mg. This particular sample size was chosen in order to lower potential variance in chemical composition between runs, as individual particles display different CaO/MgO ratios. The total gas flowrate in the furnace was maintained at 100 NmL/min using mass flow controllers. The gas compositions were switched between carbonation and calcination cycles as shown in Table 2. Based on previous testing, where CaO carbonation profiles were compared at multiple flowrates ranging from 50 to 200 NmL/min, it has been shown that the selected operating conditions limit gas diffusion resistance from the bulk gas to the particle surface.^[10,11] In addition, Perejon *et al.*^[12] performed similar testing using a gas flow rate of 50 mL/min and noted that gas diffusion resistance through the sample only becomes relevant for sample masses above 40 mg for their TGA setup.

Table 2: TGA test conditions

	Carbonation			Calciner		
Case	Temperature (°C)	Gas composition (vol.%)	Pressure (kPa(a))	Temperature (°C)	Gas composition (vol.%)	Pressure (kPa(a))
Base Case NG	730	CO ₂ -16.7% N ₂ - 76.4% H ₂ O - 6.9%	101	892	CO ₂ - 63.3% H ₂ O - 36.7%	101
Press. NG	778	CO ₂ -16.7% N ₂ - 76.4% H ₂ O - 6.9%	202	893	CO ₂ - 64.5% H ₂ O - 35.5%	101

Base Case Coal	730	CO ₂ -16.7% N ₂ - 76.4% H ₂ O - 6.9%	101	912	CO ₂ -84.8% H ₂ O - 15.2%	101
Press. Coal	778	CO ₂ -16.7% N ₂ - 76.4% H ₂ O - 6.9%	202	912	CO ₂ - 85.3% H ₂ O - 14.7%	101

The gas compositions and temperatures were selected using preliminary process simulations to identify conditions where the carbonator and calciner would operate with a minimal temperature difference. The tests simulate both natural gas and coal flue gas generated during oxy-fuel calcination. Tests were performed at atmospheric pressure and 202 kPa(a) for both simulated fuels. At atmospheric pressure, an initial 40-min calcination was performed, followed by subsequent 5-min carbonations and 5-min calcinations. When carbonating at 202 kPa(a), the carbonation duration was increased to 10 min to ensure the end of the kinetic-controlled stage of carbonation is reached. At the end of the carbonation period, the system pressure was slowly dropped to 101 kPa(a) using an automated pressure control valve which ensured the target gas composition was maintained. After calcination at atmospheric pressure, the reactive gas was switched to an inert and the pressure was increased to 202 kPa(a) *via* the same automated pressure control valve. In all cases, 20 cycles were performed on each sample.

A typical carbonation/calcination cycle is illustrated in Figure 2. Once the carbonation temperature is reached, the gas atmosphere is switched and the weight of the sample starts increasing after a short delay due to the volume of the gas lines. The carbonation is divided into two steps: a fast reaction kinetic-driven stage followed by a slower diffusion-limited stage. Appearance of the second step results from the formation of a carbonate layer at the surface of the particles through which CO₂ must diffuse before accessing unreacted CaO.^[13] After the carbonation period, the temperature is increased and the gas atmosphere switched to calcination conditions. Due to the higher CO₂ partial pressure, the sample weight increases (*via* carbonation) until a sufficiently high temperature is reached for calcination to occur; the sample temperature is raised to the calcination temperature as quickly as possible to limit its impact. The level of recarbonation in Figure 2 (first cycle) is not observed in the subsequent cycles and, therefore, does not significantly affect the activity of the sorbent, which ultimately reaches its residual value. It should be noted that this extra carbonation is unavoidable when calcining

under high CO₂ environments and has been noted by previous authors when operating at temperatures above 900°C and 70 vol.% CO₂.^[12,14] Some level of recarbonation can be expected in a real system during transfer of the sorbent to the calciner (using CO₂) and has been observed experimentally.^[15] The sample is fully calcined before the end of the calcination period, after which the temperature is reduced under pure nitrogen before initiating the next cycle.

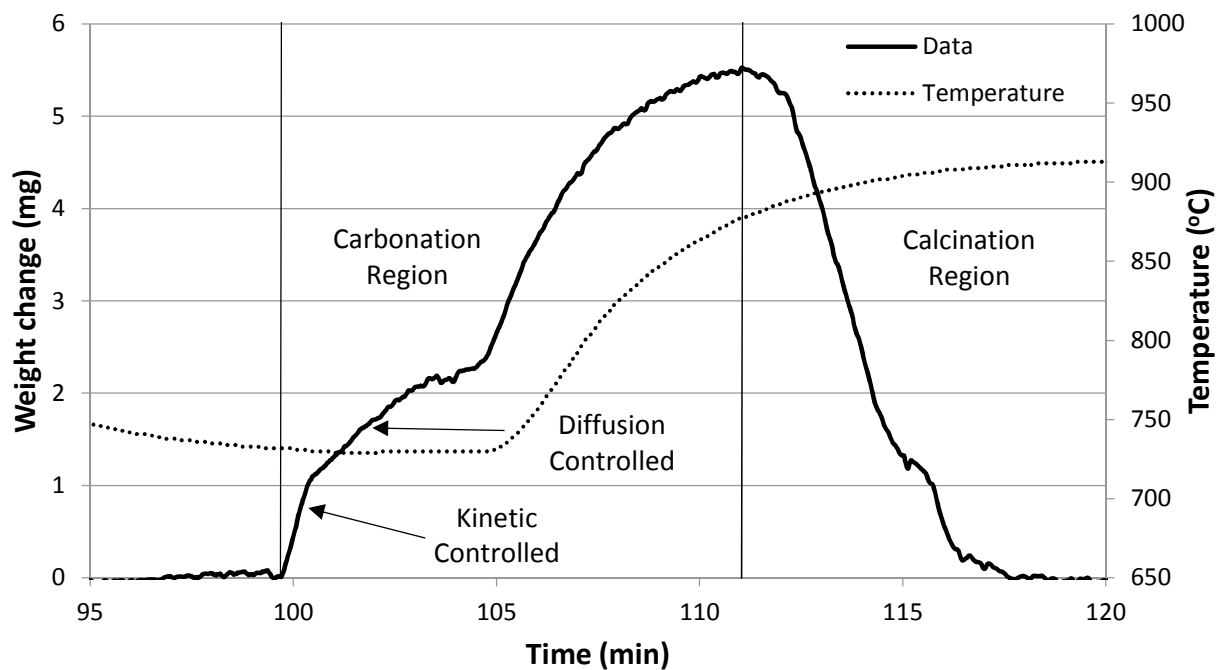


Figure 2: Sample weight and temperature vs. time for the first cycle of the simulated coal base case conditions – Carbonation in 76.4% N₂, 16.7% CO₂ and 6.9% H₂O – Calcination in 84.8% CO₂ and 15.2% H₂O. All concentrations in vol.%.

It should be noted that the CaO conversion used in this work only takes into account the first phase of the carbonation. This choice was made to reflect the shorter residence times of the particles in the circulating fluidized bed that the authors expect to be used for this CO₂ capture process. Consequently, the expected average conversions are lower than what is presented in the available literature, especially from TGA data.^[16–18]

Computational Methods

The PFBC was modeled using information from the Karita P800 boiler in Japan that was designed to produce 360 MW_e with a net efficiency of 41.8% HHV.^[6,19] The power output is split between a steam turbine (290 MW_e) and a gas turbine (70 MW_e). The key specifications of this unit are summarized in Table 3.

Table 3: Main specifications of Karita P800 from Koike *et al.*^[19]

Boiler type		Pressurized bubbling fluidized bed
Total output		360 MW _e
Gas turbine output		70 MW _e
Steam turbine output		290 MW _e
Net efficiency		41.8% HHV
Gross efficiency		42.8% HHV
Steam conditions (supercritical)		
	Pressure	24,100 kPa(a)
	Temperature	566/593°C (Main/reheat)
Gas conditions		
	Pressure	Approx. 1300 kPa
	Temperature	Approx. 850°C
De-SO_x system		In-situ with limestone

De-NO_x system	PFBC combustion + SCR ^a
Dust collector	2-stage cyclones + ESP ^b

^aselective catalytic reduction; ^belectrostatic precipitator

The fuel fed to the boiler contains a lime-based sorbent for in-situ desulphurization.^[6] The combustion takes places at 1300 kPa(a) and 850°C. A two-stage cyclone is used to reduce the particle matter concentration before sending the flue gas to the gas turbine. After the turbine, the gas is treated for NO_x using a selective catalytic reduction process (SCR) and passes through the steam cycle economizer used for boiler feed water pre-heat. A last particle removal step is carried out with an electrostatic precipitator (ESP) before sending the flue gas to the stack.

The Karita PFBC is simulated using Blair Athol coal, with proximate and ultimate analyses provided in Table 4. The total coal feed rate was adjusted to match the desired power output of 360 MW_e. Note that the total coal feed rate to the PFBC unit is directly calculated from the fuel HHV and the net efficiency of the PFBC *via* the following equation:

$$\dot{m} = \frac{P}{HHV_{coal} \cdot \eta_{net}} \quad (3)$$

where \dot{m} is the total coal feed rate, P is the desired power output, HHV_{coal} is the higher heating value of the coal, and η_{net} is the net efficiency of the PFBC unit. The sorbent feed rate is based on results from the operation of the Tidd PFBC demonstration project where a calcium-to-sulphur (Ca/S) molar ratio of 1.5 was sufficient to achieve 95% sulphur capture.^[20]

Table 4: Blair Athol coal analysis from Huleatt ^[21]

Proximate analysis			Ash analysis (wt.%)	
Moisture	wt.%	7.5	SiO ₂	61.3
Volatile matter	wt.%	27.2	Al ₂ O ₃	30.2
Fixed carbon	wt.%	57.3	Fe ₂ O ₃	4.2
Ash	wt.%	8	CaO	0.5
Total	wt.%	100	MgO	0.5
			TiO ₂	1.6
Ultimate analysis			Na ₂ O	0.2
Moisture	wt.%	7.5	K ₂ O	0.3
Carbon	wt.%	68.6	Mn ₃ O ₄	0.1
Hydrogen	wt.%	3.7	P ₂ O ₅	0.2
Nitrogen	wt.%	1.4	SO ₃	0.2
Chlorine	wt.%	0		
Sulphur	wt.%	0.3		
Ash	wt.%	8		
Oxygen	wt.%	10.5		
Total	wt.%	100		
Calorific analysis (HHV, air dried)	MJ/kg	27.28		

Combustion air is compressed from atmospheric pressure to 1300 kPa(a), with an assumed composition of 79 vol.% nitrogen and 21 vol.% oxygen. Following the quality guidelines for

energy system studies suggested by NETL,^[22] the stage pressure ratio is limited to 2.5, meaning that a three-stage compressor is required. Inter-stage cooling is implemented so that the discharge air temperature from each stage does not exceed 167°C.^[23] A 2% pressure drop based on the inlet pressure is assumed for each inter-stage cooler.^[22] The boiler is simulated using the Peng-Robinson equation of state and a Gibbs reactor with a combustion efficiency of 99.5% to match the performance of the Tidd unit.^[20] The isentropic efficiency of the turbine is calculated by reproducing the Karita unit performance. The efficiency is adjusted until the power output from the gas turbine is 70 MW_e, resulting in an isentropic efficiency of 88%. For the present work, the efficiency calculated above is adopted for all gas turbines in the simulation. The discharge pressure is set to 121.3 kPa(a), to account for an assumed pressure drop of 20 kPa in the calcium looping carbonator. The mechanical efficiency of the turbine is set at 98.5%.^[22] The output from the gas turbine is then fed to the CaL capture cycle as illustrated in Figure 3.

Process simulations were performed using aspenONETM, with the base cases including the use of both coal and natural gas as fuels for the calciner. Between these two simulations, all the operating conditions were identical, with the exception of the fuel due to the presence of sulphur and ash for the coal cases. The sulphur causes a slight increase in the CaO circulation rate from the irreversible formation CaSO₄. Note that the influence of ash on sorbent conversion is not considered here and is assumed negligible based on low measured cyclic conversions and relatively high sorbent make-up rates. In the simulation, the ash increases the amount of inert solids in the process, leading to higher fuel consumption. Base case simulation parameters for natural gas and coal cases are presented in Table 5 where F_0 and F_{CO_2} are defined as the molar flow of CaCO₃ in the make-up stream and the molar flowrate of CO₂ in the flue gas entering the carbonator, respectively. The reactors operate at atmospheric pressure and at temperatures corresponding to the experiments conducted and presented in the experimental section. Conversion of the CaO in the carbonator is tied to the solids circulation rate, the make-up rate, and the sorbent properties.

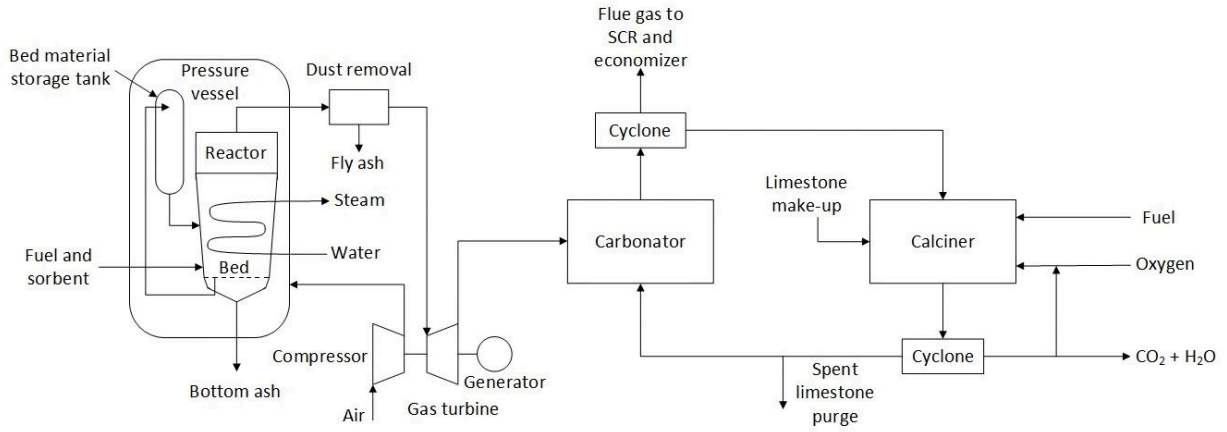


Figure 3: PFBC-CaL process flow diagram

Table 5: Base case simulation parameters

Parameter/Fuel	Carbonator Temperature	Calciner Temperature	Reactor Pressure Drop	Make-up Ratio (F_0/F_{CO_2})	Carbon Intensity (kg CO_2 /MW _e h)
NG	730°C	892°C	20 kPa	0.05	420
Coal	730°C	912°C	20 kPa	0.12	420

Due to the sorbent deactivation during particle cycling, an estimation of the particle residence time in the process is required. In addition, the following equation is utilized to predict the particle conversion, X_N , over a large number of process cycles, N :^[24]

$$X_N = \frac{1}{\frac{1}{1-X_r} + kN} + X_r \quad (4)$$

where k is a decay parameter and X_r is the residual conversion at high cycle numbers. The average conversion of all the solids in the carbonator, X_{ave} , is a weighted average over the cycle numbers:^[25]

$$X_{ave} = \sum_N r_N X_N \quad (5)$$

$$r_N = \frac{F_0 F_R^{N-1}}{(F_0 + F_R)^N} \quad (6)$$

where r_N represents the fraction of particles of age N , F_R is the molar flow rate of CaO entering the carbonator. The sum in Equation (5) is an infinite sum. During this study, enough cycles have been considered to account for over 95% of the solids ($\sum_N r_N \geq 0.95$). The make-up rate of limestone (Equation (7)) and the circulation of calcium oxide (Equation (8)) are both defined as ratios based on flue gas CO₂ entering the CaL process:

$$\frac{F_0}{F_{CO_2}} \quad (7)$$

$$\frac{F_R}{F_{CO_2}} \quad (8)$$

All cases are simulated under conditions that meet the Canadian carbon emissions regulations currently in place.^[3] No hydrodynamic modeling of the carbonator has been included, instead the carbonator is assumed to be perfectly mixed and the partial pressure of the CO₂ leaving the reactor is at equilibrium conditions. Therefore, the carbonator CO₂ capture efficiency was dependant on the carbonator temperature and varied based on operating pressure. The amount of circulating CaO and the fuel feed rate are calculated so that the calciner does not produce additional heat (*i.e.*, only enough heat for calcination) and to meet the carbon intensity specification. The production of oxygen (99 vol.%) is not simulated and the air separation unit (ASU) energy consumption is calculated from a specific energy consumption of 231 kWh/tonne O₂.^[26] The oxygen is fed in excess to maintain 2.7 vol.% O₂ (dry basis) in the gas outlet of the calciner.^[22]

Calciner flue gas recycling is implemented to maintain fluidization conditions and reduce the oxygen concentration in the fluidization gas. While the process simulation does not include a hydrodynamic model or sizing of the calciner, the recycle ratio is set to achieve 30 vol.% O₂ concentration at the reactor windbox, in alignment with the base case of the US Department of Energy (DOE) experimental work.^[26] In all cases, the calcination conversion was fixed at 100%. The recycled flue gas stream is cooled to limit the blower inlet temperature to 190°C. The blower compensates for the calciner pressure drop and increases the gas stream pressure by 20 kPa. The energy required to condition and compress the concentrated CO₂ stream is calculated using a 5-stage compression process with inter-stage cooling. The condensate collected after each cooling step is separated before sending the gas phase to the next compression stage. The CO₂ stream is compressed in this manner until condensation occurs at

20°C, after which the CO₂ is pumped to a final pressure of 15000 kPa(a). A dedicated sub-critical steam cycle is used to recover energy from the capture process and produce additional power. The gross efficiency of that cycle was calculated to be 35% (HHV) in previous work,^[9] and has been employed here.

RESULTS

Limestone Conversion

As discussed in the experimental method section above, only sorbent performance during the initial rapid carbonation stage is important, since marginal improvements in carbonation conversion are realized after this point. The end of this stage is approximated by the intersection of two linear regressions for each of the carbonation stages. The results presented here illustrate the decay of the sorbent conversion with repeated process cycles. The emphasis is on conversion at high cycle numbers, since high make-up ratios are not desirable from an economic perspective unless the spent lime can be used for cement applications for example which is outside of the remit for this paper. Results from the experimental tests simulating the use of natural gas for calcination are presented in Figure 4. It was observed that operating the carbonation at a higher pressure results in higher conversion, due largely to the higher CO₂ partial pressure. The improvement over the results at atmospheric pressure tend to be reduced at higher cycle numbers, although the predicted values for residual conversions are still higher under pressurized conditions (Table 6). This is an important result since conversion predictions at high cycle numbers greatly affect process performance.

The experiments simulating coal combustion for sorbent calcination show a similar behaviour (Figure 5). The higher CO₂ partial pressures result in higher conversions at all cycle numbers (Table 6). Comparing coal and natural gas conditions, we can see that natural gas calcination conditions are slightly more favourable in terms of CaO conversion, likely due to a combination of lower operating temperature and the presence of steam. While the individual effects of these two parameter are not tested here, they have both been tested independently elsewhere and shown to increase CaO conversion.^[16, 27] Although, the natural gas conditions result in marginally better CaO conversions, both sets of calcination conditions give relatively low cyclic conversions, even over the first few cycles. As noted above, the recorded CaO conversions are taken at the end of the kinetic-controlled stage and partially explain the reduced cyclic carrying capacity. In addition, calcination takes place under high CO₂ partial pressures and elevated temperatures, which are known to increase particle sintering, limiting particle porosity, and dramatically decreasing the rate of carbonation. Perejon *et al.*^[12] and Ortiz *et al.*^[14] have noted that the traditional equations for calculating CaO conversion do not reflect the effect of calcination under high CO₂ partial pressures, as would be the case in the CaL technologies, and that the solid-state diffusion controlled carbonation is “greatly enhanced”

when CaO is regenerated under high CO₂ partial pressures as compared to calcination under low CO₂ concentration. Their results showed CaO conversions, at the end of the reaction-controlled stage, of ~4% after 20 cycles and residual conversions of <3% under similar conditions as the present work. In addition, these low residual activities are in-line with carbonation performance observed during pilot-scale trials with the same sorbent.^[15]

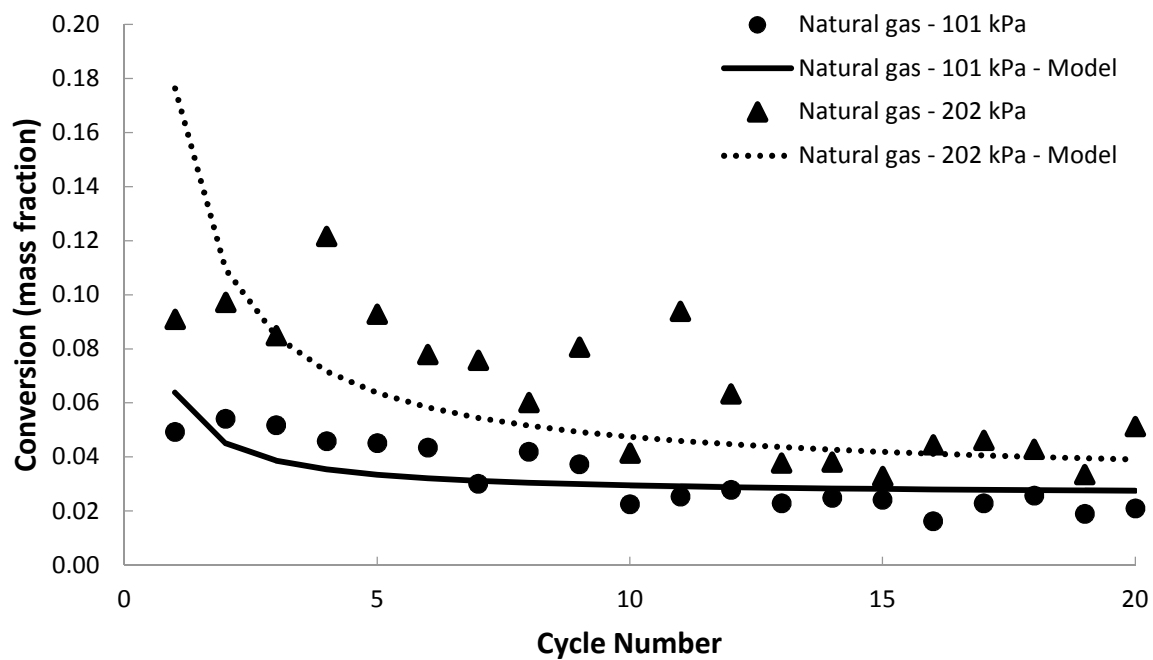


Figure 4: Sorbent conversion vs. process cycle number – Simulated natural gas flue gas conditions.

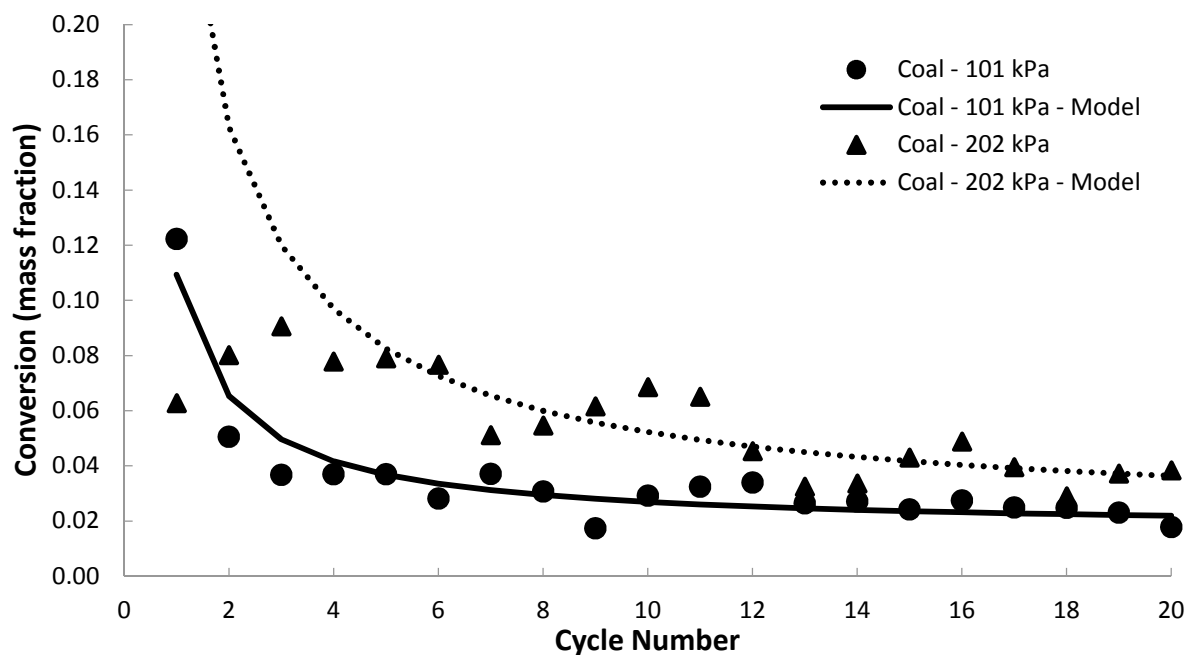


Figure 5: Sorbent conversion vs. process cycle number – Simulated coal flue gas conditions.

The conversion decay model presented in the experimental method section was fitted to all four sets of data, with the resulting model parameters presented in Table 6. Particular attention has been given to how well the model fits the higher cycle number data points (>10 cycles) due to the importance of high cycle number on system performance. While complete data sets obtained at atmospheric pressure were used during model fitting, the two pressurized data sets were fitted based only on the last 10 to 15 cycle data points. This decision was made based on the significant variability in sorbent conversion, which is thought to be due to greater water throughput. With increased water injection rates to the system, the likelihood of incomplete vapourization in the feed line increases, allowing liquid to enter the TGA. The authors believe this rapid vapourization caused a perturbation in the gas flow around the sample, causing a significant amount of noise in the recorded sample weight. Although the decay model provides a poor fit for the first few cycles, this does not affect the subsequent modeling results since the average sorbent conversion of all the solids in the carbonator is effectively equal to the residual conversion.

Table 6: Sorbent conversion model parameters

	Natural gas cases		Coal cases	
	P = 101 kPa	P = 202 kPa	P = 101 kPa	P = 202 kPa
X_r	0.026	0.031	0.017	0.020
k	25.012	5.832	9.792	2.994

Process Simulations

The results of the base case simulations for atmospheric pressure natural gas calcination are shown in Table 7. Process performance metrics are presented for two distinct scenarios: (1) where the current regulation is targeted (*i.e.*, the power required by the CO₂ processing unit (CPU) is left out of the energy penalty); and (2) a more stringent case where the compression of CO₂ is accounted for in the CO₂ intensity calculations. The focus of the discussion will be on scenario (1), but results from both are presented.

Table 7: Base case simulations – Natural gas – PFBC-CaL process performance summary with and without the CPU included in target CO₂ emissions intensity

		With CPU	Without CPU
PFBC	Net power (MW _e)	360.0	360.0
	Efficiency (% HHV)	41.8	41.8
CaL Process	Thermal input (MW _{th})	490.8	461.3
	CaL assumed gross efficiency (% HHV)	35.0	35.0
	CaL gross power (MW _e)	171.8	161.5
	Auxiliaries (MW _e)	11.8	11.1
	CPU (MW _e)	21.2	20.0
	ASU (MW _e)	32.1	30.2
	Net power (MW _e)	106.7	100.2
	Efficiency (% HHV)	21.7	21.7
	Solids flow rate (kg/s)	1212.1	1132.4
	CaO conversion (%)	2.6	2.6
Global Process	Global net power (MW _e)	466.7	460.2
	Global efficiency (% HHV)	34.5	34.8
	Energy penalty (% HHV)	7.3	7.0
	CO ₂ intensity (kg CO ₂ /MW _e h)	420.0	420.0

The simulated CaL capture process produces an additional 161.5 MW_e of power (gross) of which 26% is consumed to produce oxygen and drive the process auxiliaries. The overall efficiency, grouping both the capture process and the power plant, was calculated to be 34.8%. This represents an energy penalty of 7.0 percentage points over the base power plant efficiency (41.8%). Due to the low sorbent make-up ratio selected for the base case, the sorbent particles are cycled a large number of times and the resulting average conversion reaches the residual conversion of 2.6%, as determined experimentally. This low cyclic conversion results in a relatively high solid circulation rate (1132 kg/s). In terms of loading, a 2.6% cyclic conversion equates to a capture rate of 20.4 g CO₂/kg sorbent. Although it does not compare favourably to amine absorption (17.6-40.5 g CO₂/kg solvent)^[28] or zeolite adsorption (37.4-48.4),^[29] the

carbonation of the limestone in the simulation only accounts for the fast carbonation phase, as explained in the experimental methods section.

The use of coal to provide thermal energy for calcination was also investigated (Table 8). In this case, the sorbent make-up ratio was adjusted to control the circulating ash in the process. The ash leaving the process in the purge stream causes higher purge/make-up flows to limit ash accumulation in the system. In the base case, ash represents 15 wt.% of the circulating solids at a make-up ratio of 0.12. In addition to ash impeding access to the active CaO sites, the presence of sulphur also results in the formation of CaSO₄. Together, the ash and CaSO₄ contribute to the overall solids circulation. Compared to the natural gas case, the solids circulation rate is significantly increased due to the presence of these inert solids and the lower average sorbent conversion.

Using coal also causes a larger disparity between the current CO₂ emissions intensity regulation and the more stringent cases. Due to a larger volume of CO₂, the power used to run the CPU increases and the difference in energy penalty between the two capture targets increases from 0.3 (natural gas case) to 0.9 percentage points. The absolute energy penalty of the capture process is also higher for coal *via* increased oxygen consumption and total CPU demands.

Table 8: Base case simulations – Coal – PFBC-CaL process performance summary with and without the CPU included in target CO₂ emissions intensity

		With CPU	Without CPU
PFBC	Net power (MW _e)	360.0	360.0
	Efficiency (% HHV)	41.8	41.8
CaL Process	Thermal input (MW _{th})	585.9	513.1
	CaL Assumed gross efficiency (% HHV)	35.0	35.0
	CaL Gross power (MW _e)	205.1	179.6
	Auxiliaries (MW _e)	15.8	13.8
	CPU (MW _e)	45.1	39.5
	ASU (MW _e)	53.7	47.0
	Net power (MW _e)	90.5	79.3
	Efficiency (% HHV)	15.4	15.4
	Solids flow rate (kg/s)	1983.5	1737.2
	CaO conversion (%)	2.1	2.1
	F ₀ /F _{CO2}	0.14	0.12
Global Process	Global net power (MW _e)	450.5	439.3
	Global efficiency (% HHV)	31.1	32.0
	Energy penalty (% HHV)	10.7	9.8
	CO ₂ intensity (kg CO ₂ /MW _e h)	420.0	420.0

A sensitivity analysis on the sorbent make-up ratio, which significantly influences the economics of the process, ^[30] was performed to evaluate its impact on process performance. The make-up rate, F_0 , was varied from 0.01 to 0.1, while adjusting the overall solids circulation rate to meet the specified carbon emissions intensities. The results of this analysis for the natural gas calcination cases are provided in Table 9.

Table 9: Sensitivity analysis – Sorbent make-up ratio – Natural gas cases with and without the CPU included in target CO₂ emissions intensity

With CPU	Without CPU
----------	-------------

	$F_0 =$ 0.01	$F_0 =$ 0.025	$F_0 =$ 0.05	$F_0 =$ 0.075	$F_0 =$ 0.1	$F_0 =$ 0.01	$F_0 =$ 0.025	$F_0 =$ 0.05	$F_0 =$ 0.075	$F_0 =$ 0.1
Solids flow rate (kg/s)	1261.2	1241.8	1212.1	1184.3	1157.6	1186.4	1165.1	1132.4	1101.4	1071.5
CaO conversion (%)	2.57	2.60	2.64	2.68	2.72	2.58	2.61	2.65	2.69	2.73
Global process net power (MW _e)	463.7	464.8	466.7	468.6	470.6	457.7	458.6	460.2	461.9	463.6
Global process efficiency (% HHV)	34.7	34.7	34.5	34.4	34.2	35.0	34.9	34.8	34.7	34.5
Energy penalty (% HHV)	7.1	7.1	7.3	7.4	7.6	6.8	6.9	7.0	7.1	7.3
CO ₂ intensity (kg CO ₂ /MW _e h)	420.0	420.0	420.0	420.0	420.0	420.0	420.0	420.0	420.0	420.0

Higher sorbent make-up ratios result in higher sorbent conversion and lower solids circulation rates, as a large portion of the particles are cycled fewer times. However, fuel and oxygen consumptions increase in order to heat the make-up stream to the calciner temperature and provide the necessary heat for calcination of the fresh limestone. Consequently, additional power is generated from the CaL capture process and the proportion of low-efficiency power increases in the overall system. This ultimately increases the energy penalty at higher sorbent make-up ratios.

For the coal cases, the sensitivity analysis is presented in terms of ash content in the circulating solids (Table 10). To reduce the ash content of the solid stream, a higher purge rate and, hence, a higher make-up ratio are required. The same effect on sorbent conversion and solid circulation rate is then observed. In this case, however, due to the range in which the make-up ratio is modified, a point is reached where the energy penalty is minimized (~15 wt.% ash content). At lower ash contents, the energy required to heat and calcine the fresh limestone becomes prohibitive. At higher ash contents, the amount of inert solids circulating in the

capture process significantly increases the fuel and oxygen demands *via* sensible heating demands, resulting in higher penalties.

Operating the carbonator at elevated pressures has been shown to increase the sorbent utilization potential. Considering the challenges with the transfer of solids between reactors operating at different pressures, a case with the carbonator operating at 202 kPa(a) was simulated. This is expected to be feasible since this minimal pressure difference should be easily controlled in the transfer lines. A major benefit realized by operating at elevated pressures is that the vitiated flue gas leaving the carbonator can be expanded for additional power generation. Under these conditions, the power produced by the power plant gas turbine is reduced due to the higher discharge pressure, but is more than made up for by the expander downstream of the carbonator. The total power produced from the combination of two turbines is higher than in the base case, as the carbonator acts as a reheat for the flue gas before the final expansion. The cost of the additional turbine, and its ultimate impact on the cost of electricity, should be addressed in future economic studies.

Table 10: Sensitivity analysis – Circulating solids ash content – Coal cases with and without the CPU included to obtain the target CO₂ emissions intensity

	With CPU				Without CPU			
	Ash = 5 wt.%	Ash = 10 wt.%	Ash = 15 wt.%	Ash = 20 wt.%	Ash = 5 wt.%	Ash = 10 wt.%	Ash = 15 wt.%	Ash = 20 wt.%
Solids flow rate (kg/s)	1242.3	1726.7	1983.5	2181.9	1049.3	1503.4	1737.2	1912.6
CaO conversion (%)	3.05	2.28	2.08	1.98	3.05	2.28	2.08	1.98
F ₀ /F _{CO2}	0.50	0.21	0.14	0.10	0.42	0.19	0.12	0.09
Global net power (MW _e)	446.9	446.3	450.5	455.3	433.4	435.2	439.3	443.6
Global efficiency (% HHV)	30.0	31.0	31.1	31.1	31.1	31.9	32.0	31.9
Energy penalty (% HHV)	11.84	10.78	10.67	10.75	10.7	9.9	9.8	9.9
CO ₂ intensity (kg CO ₂ /MW _e h)	420.0	420.0	420.0	420.0	420.0	420.0	420.0	420.0

For both the natural gas and coal cases, the effect of increasing the carbonator operating pressure is beneficial on multiple fronts, as shown in Tables 11 and 12. Increasing the power output from the turbines reduces the amount of CO₂ requiring capture to reach the regulation target. In addition, the fuel demand is significantly reduced, along with oxygen consumption and power requirements for auxiliaries and CO₂ processing. Sorbent conversions under pressurized conditions are higher, which contributes to the reduction in solids circulation and lowers the capture level requirement. In the natural gas case, pressurization lowers the circulating rate; however, this is not the case for coal since the make-up ratio is reduced at higher pressure to maintain the 15% ash content, causing an increase in the solids flow rate.

Table 11: Sensitivity analysis – Pressure – Natural gas cases with and without the CPU included in the target CO₂ emissions intensity

		With CPU		Without CPU	
		P = 101 kPa	P = 202 kPa	P = 101 kPa	P = 202 kPa
CaL process	Thermal input (MW _{th})	490.8	368.9	461.3	347.3
	CaL Assumed gross efficiency (% HHV)	35.0%	35.0%	35.0%	35.0%
	CaL Gross power (MW _e)	171.8	129.1	161.5	121.6
	Auxiliaries (MW _e)	11.8	8.9	11.1	8.4
	CPU (MW _e)	21.2	19.1	20.0	18.0
	ASU (MW _e)	32.1	24.3	30.2	22.8
	Net power (MW _e)	106.7	76.9	100.2	72.3
	Efficiency (% HHV)	21.7%	20.8	21.7%	20.8
	Solids flow rate (kg/s)	1212.1	955.9	1132.4	890.2
	CaO conversion	2.6%	3.5%	2.6%	3.6%
Global process	Global net power (MW _e)	466.7	457.2	460.2	452.8
	Global efficiency (% HHV)	34.5%	37.2%	34.8%	37.5%
	Energy penalty (% HHV)	7.3%	7.0%	7.0	6.7%
	CO ₂ intensity (kg CO ₂ /MW _{e,h})	420.0	420.0	420.0	420.0

Table 12: Sensitivity analysis – Pressure – Coal cases with and without the CPU included in the target CO₂ emissions intensity

With CPU		Without CPU	
P = 101 kPa	P = 202 kPa	P = 101 kPa	P = 202 kPa

CaL process	Thermal input (MW _{th})	585.9	482.4	513.1	426.7
	CaL Assumed gross efficiency (% HHV)	35.0	35.0	35.0	35.0
	CaL Gross power (MW _e)	205.1	168.9	179.6	149.3
	Auxiliaries (MW _e)	15.8	13.0	13.8	11.5
	CPU (MW _e)	45.1	39.0	39.5	34.5
	ASU (MW _e)	53.7	44.3	47.0	39.2
	Net power (MW _e)	90.5	72.5	79.3	64.2
	Efficiency (% HHV)	15.4	15.0	15.4	15.0
	Solids flow rate (kg/s)	1983.5	2063.6	1737.2	1825.0
	CaO conversion (%)	2.08	2.01	2.08	2.01
	F ₀ /F _{CO2}	0.14	0.11	0.12	0.10
Global process	Global net power (MW _e)	450.5	448.9	439.3	440.9
	Global efficiency (% HHV)	31.1	33.4	32.0	34.2
	Energy penalty (% HHV)	10.7	10.3	9.8	9.5
	CO ₂ intensity (kg CO ₂ /MW _{eh})	420.0	420.0	420.0	420.0

CONCLUSIONS

Cadomin limestone performance for CaL-based CO₂ capture was investigated in a TGA using relatively high-temperature carbonation and low-temperature calcination. Considering only the first fast phase of carbonation, the sorbent was exposed to conditions representing both natural gas and coal combustion flue gases. In addition, sorbent performance at elevated pressure carbonation conditions was investigated. The results showed residual sorbent conversions ranging from 2 to 3%, with simulated coal flue gas achieving lower conversions than those of natural gas.

A CaL-based CO₂ capture process was modeled using process simulation software to assess the impact of post-combustion CO₂ capture, using both natural gas and coal, on the efficiency of a PFBC power plant. Natural gas performance was superior in all cases due primarily to the absence of ash and CaSO₄, which led to higher solids circulation rates and energy penalties. A sensitivity analysis on the sorbent make-up ratio was investigated. In the case of natural gas, a reduction in solids circulation was observed, ultimately increasing the energy penalty *via* fresh sorbent heating demands. On the other hand, coal cases showed a minimum energy penalty at around 15 wt.% ash content. Increasing the operating pressure of the carbonator was beneficial from both an energy penalty and solids circulation perspective, with the exception of the coal case where maintaining the same ash content requires a lower sorbent make-up ratio; thus, causing a higher circulation rate.

ACKNOWLEDGEMENT

This research was sponsored and funded by the Program for Energy Research and Development (PERD) at Natural Resources Canada, Government of Canada.

REFERENCES

- [1] International Energy Agency, "Key World Energy Statistics," IEA, **2017**, accessed on 10 August 2018, <https://www.iea.org/publications/freepublications/publication/KeyWorld2017.pdf>.
- [2] International Energy Agency, "CO₂ Emissions from Fuel Combustion - Highlights," IEA **2017**, accessed on 10 August 2018, <https://www.iea.org/publications/freepublications/publication/CO2EmissionsfromFuelCombustionHighlights2017.pdf>.
- [3] Government of Canada, "Regulations Limiting Carbon Dioxide Emissions from Natural Gas-fired Generation of Electricity," Canada Gazette, **2018**, accessed on 10 August 2018, <http://gazette.gc.ca/rp-pr/p1/2018/2018-02-17/html/reg4-eng.html>.
- [4] Environment and Climate Change Canada, "Technical Backgrounder: Proposed Federal Regulations for Electricity Sector," Government of Canada, **2018**, accessed on 10 August 2018, https://www.canada.ca/en/environment-climate-change/news/2018/02/technical_backgrounderproposedfederalregulationsforelectricityse.html.
- [5] M. Alvarez Cuenca, E. J. Anthony, Pressurized Fluidized Bed Combustion, 1st edition, Springer Science and Business Media, Dordrecht **1995**.
- [6] M. Hirota, *Japan Soc. Mech. Eng. Int. J.* **2004**, 47, 193.
- [7] G. S. Grasa, M. Alonso, J. C. Abanades, *Ind. Eng. Chem. Res.* **2008**, 47, 1630.
- [8] C. Luo, Y. Zheng, J. Guo, B. Feng, *Fuel* **2014**, 127, 124.
- [9] B. Duhoux, P. Mehrani, D. Y. Lu, E. J. Anthony, R. Symonds, A. Macchi, *Energy Tech.* **2016**, 4, 1158.
- [10] R. T. Symonds, D. Y. Lu, R. W. Hughes, E. J. Anthony, A. Macchi, *Chem. Eng. Sci.* **2009**, 64, 3536.
- [11] R. T. Symonds, D. Y. Lu, A. Macchi, R. W. Hughes, E. J. Anthony, *Chem. Eng. Sci.* **2017**, *In Press*.
- [12] A. Perejon, J. Miranda-Pizarro, L. A. Perez-Maqueda, J. M. Valverde, *Energy* **2016**,

113, 160.

- [13] S. K. Bhatia, D. D. Perlmutter, *AIChE J.* **1983**, 29, 79.
- [14] C. Ortiz, R. Chacartegui, J. M. Valverde, J. A. Becerra, L. A. Perez-Maqueda, *Fuel* **2015**, 160, 328.
- [15] R. T. Symonds, S. Champagne, F. Ridha, D. Lu., *Powder Technol.* **2016**, 290, 124.
- [16] S. Champagne, D. Y. Lu, A. Macchi, R. T. Symonds, E. J. Anthony, *Ind. Eng. Chem. Res.* **2013**, 52, 2241.
- [17] F. Donat, N. H. Florin, E. J. Anthony, P. S. Fennell, *Environ. Sci. Technol.* **2012**, 46, 1262.
- [18] V. Manovic, E. J. Anthony, *Energy & Fuels* **2010**, 24, 5790.
- [19] J. Koike, S. Nakamura, H. Watanabe, T. Imaizumi, "Manufacturing and construction, operation of Karita PFBC 360 MW unit," 17th International Conference on Fluidized Bed Combustion, American Society of Mechanical Engineers, Jacksonville, 15 June **2003**
- [20] US DOE - NETL, "Tidd PFBC demonstration project: Project performance summary," DOE, **1999**, accessed on 10 August 2018, <https://www.netl.doe.gov/File%20Library/Research/Coal/major%20demonstrations/cctdp/Round1/TIDD/TIDD1.pdf>
- [21] M. B. Huleatt, "Handbook of Australian black coals : geology, resources, seam properties, and product specifications," Australian Government, **1991**, accessed on 10 August 2018, <https://data.gov.au/dataset/572b6e69-1489-454b-b0c2-f6cdf5bac6dc>
- [22] US DOE - NETL, "Quality guidelines for energy system studies - Process modeling design parameters", DOE/NETL, **2014**, accessed on 10 August 2018 https://www.netl.doe.gov/energy-analyses/temp/QGESSProcessModelingDesignParameters_042514.pdf.
- [23] R. Turton, R. C. Bailie, W. B. Whiting, J. A. Shaeiwitz, D. Bhattacharyya, Analysis, Synthesis, and Design of Chemical Processes, 4th edition, Prentice Hall, Boston, **2012**.
- [24] G. S. Grasa, J. C. Abanades, *Ind. Eng. Chem. Res.* **2006**, 45, 8846.

- [25] J. C. Abanades, *Chem. Eng. J.* **2002**, *90*, 303.
- [26] N. Y. Nsakala, G. N. Liljedahl, "Greenhouse gas emissions control by oxygen firing in circulating fluidized bed boilers: Phase 1 - A preliminary systems evaluation," Alstom Power Inc., **2003**, accessed 10 August 2018, <https://www.osti.gov/servlets/purl/825796>.
- [27] M. Broda, A. M. Kierzkowska, C. R. Müller, *Environ. Sci. Technol.* **2012**, *46*, 10849.
- [28] Y. Du, Y. Yuan, G. T. Rochelle, *Chem. Eng. Sci.* **2016**, *155*, 397.
- [29] R. Chatti, A. K. Bansawal, J. A. Thote, V. Kumar, P. Jadhav, S. K. Lokhande, *Microporous Mesoporous Mater.* **2009**, *121*, 84.
- [30] L. M. Romeo, Y. Lara, P. Lisbona, J. M. Escosa, *Chem. Eng. J.* **2009**, *147*, 252.

Simulation of a calcium looping CO₂ capture process for pressurized fluidized bed combustion

Duhoux, Benoit

2019-06-05

Attribution-NonCommercial 4.0 International

Duhoux B, Symonds RT, Hughes R, et al., (2020) Simulation of a calcium looping CO₂ capture process for pressurized fluidized bed combustion. Canadian Journal of Chemical Engineering, Volume 98, Issue 1, January 2020, pp. 75-83

<https://doi.org/10.1002/cjce.23569>

Downloaded from CERES Research Repository, Cranfield University